Structural and magnetic properties of the $Ni_5Ti(O_2BO_3)_2$ ludwigite

M. A. V. Heringer,[1] D. C. Freitas,[1] D. L. Mariano,[1] E. Baggio-Saitovitch,[2] M. A. Continentino,[2] and D. R. Sánchez[1,*]

[1]*Instituto de Física, Universidade Federal Fluminense, Campus da Praia Vermelha, 24210-340, Niterói, Rio de Janeiro, Brazil*

[2]*Centro Brasileiro de Pesquisas Física, Rua Doutor Xavier Sigaud, 150-Urca 22290-180 Rio de Janeiro, Rio de Janeiro, Brazil*

(Received 11 April 2019; published 5 September 2019)

This work presents a study of the oxyborate $Ni_5Ti(O_2BO_3)_2$ using single-crystal x-ray diffraction and magnetic and specific-heat measurements. This material has in its crystalline structure subunits in the form of three-legged ladders. Despite the magnetic ions occupying these low-dimensional structures, we find that this system has long-range magnetic order at low temperatures. The analysis of the magnetization and specific-heat data shows that the process of establishing this order is complex and occurs in several stages upon lowering the temperature. Initially at 92 K a partial magnetic ordering of the Ni moments in one of the two ladders sets in. As the system is further cooled, weakly coupled clusters of spins order, and, finally, at 78 K the whole system of spins in the two ladders are magnetically ordered. Since the Ti ions are found in the nonmagnetic valence state Ti^{4+}, the magnetic order is exclusively due to the Ni^{2+} ions with spin $S = 1$. We discuss the ferrimagnetic nature of the long-range order, which is consistent with our knowledge of the magnetic interactions, the atomic distances, and bond angles obtained from the x-ray data.

DOI: 10.1103/PhysRevMaterials.3.094402

I. INTRODUCTION

Oxyborates are examples of strongly correlated electron systems with many interesting physical properties. In particular, the ludwigites with general formula $M_2^{2+}M'^{3+}O_2BO_3$ (M, M' = transition metal) present a variety of behavior, such as low-dimensional magnetism [1,2], charge ordering [3], long-range magnetic order [3,4], spin-glass-type order [5], the coexistence of magnetic order and paramagnetism [6], the magnetocaloric effect [7], dynamic magnetism coexisting with partial magnetic ordering [3], and structural ordering [3], among others. Until now, the mechanisms responsible for many of these properties have not been fully identified. On the other hand, it is generally accepted that an understanding of the physical properties of the ludwigites requires taking into account the existence of low-dimensional subunits in its crystalline structure. They consist of two types of three-legged ladders (see Fig. 1), as will be discussed below.

Among the most studied ludwigites are the only two known homometallic members of this family; namely, $Co_3O_2BO_3$ [8] and $Fe_3O_2BO_3$ [3]. Both compounds present long-range magnetic order at low temperatures. They also have in common the presence of metallic ions with mixed-valence states 2+ and 3+ associated with different spins. This leads to a strong competition between direct- super-, and double-exchange interactions. The combination of this competition with the low dimensionality of the underlying magnetic structure characteristic of these materials seems to be the main factor that determines their complex magnetic arrangements [1–4,6].

To better understand the magnetic, thermodynamic, and structural properties of homometallic ludwigites, these compounds were doped with different metallic ions [4–7]. When the dopants are magnetic metallic ions, in general, there is not a real thermodynamic magnetic transition when the system is cooled. For example, in both heterometallic Co_2FeBO_5 and Ni_2FeBO_5 ludwigites, it is possible to observe ordering of only one magnetic component; namely, that of the subsystem formed by Fe^{3+} ions. The behavior of the magnetic moments of the complementary ions (Co^{2+} or Ni^{2+}) is complex at low temperatures [6]. Also, when doped with nonmagnetic ions, such as Ti^{4+}, Mg^{2+}, Ga^{3+}, Ge^{3+}, forming heterometallic ludwigites such as $Co_5Ti(O_2BO_3)_2$ [5] and $CoMgGaO_2BO_3$ [9], long-range magnetic order is, in general, destroyed and a spin-glass state sets in at low temperatures. However, when the $Co_3O_2BO_3$ ($T_N = 42$ K) ludwigite is doped with the nonmagnetic ion Sn, forming $Co_5Sn(O_2BO_3)_2$ [4], surprisingly the magnetic interactions are strengthened and the critical temperature for appearance of long-range magnetic order is raised up to 82 K [4]. This is the highest magnetic transition temperature, observed for the entire system, among these ludwigites. The suppression of the double-exchange interaction in the doped sample was recognized as being responsible for the increase of the magnetic transition temperature [4].

On the other hand, the ludwigites that have as main component the metallic ion Ni have been less studied. We must mention here that the existence of the homometallic ludwigite $Ni_3O_2BO_3$ has never been reported. Thus, all Ni ludwigites found in the literature are heterometallic with the general formula $Ni_2M'O_2BO_3$ where M' is a transition-metal ion. Among the most studied are the ludwigites with M' being a magnetic ion: $Ni_2FeO_2BO_3$ [6] and $Ni_2MnO_2BO_3$ [10]. In $Ni_2FeO_2BO_3$ the subsystem formed by the Fe^{3+} ions is magnetically ordered around 112 K. The other subsystem formed by Ni^{2+} divalent ions does not exhibit long-range magnetic order and seems to freeze at lower temperatures [6]. $Ni_{1.2}Mn_{1.8}BO_5$ undergoes a magnetic transition at 92 K and the effect of magnetization-sign reversal was observed in

*dalbersanchez@id.uff.br

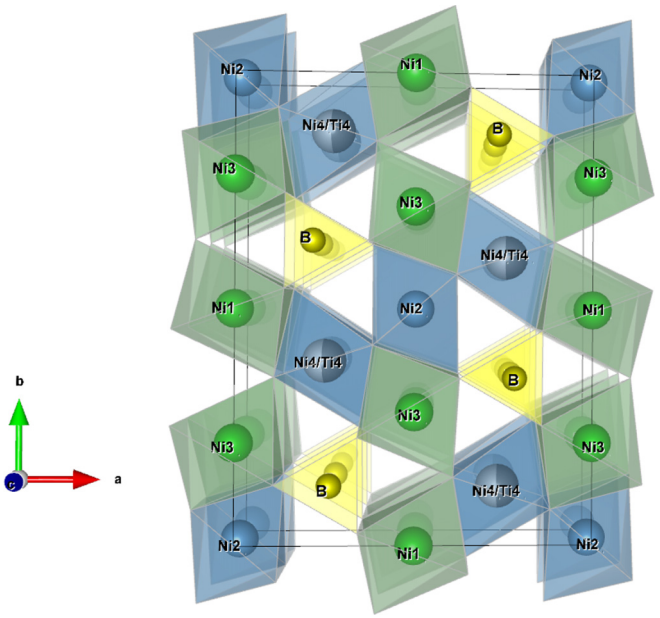

FIG. 1. Perspective view of the $Ni_5Ti(O_2BO_3)_2$ ludwigite structure. The continuous line represents the unitary cell. The metallic ions occupy sites along two three-legged ladders that extend along the c axis. These ladders are formed by sites 3-1-3 and 4-2-4, respectively, and behave as two weakly coupled, nearly independent subunits. This figure was generated by VESTA software [15].

this compound when the magnetization becomes negative or opposite to the applied magnetic field [11]. The appearance of this effect comprises different temperature dependencies of sublattice magnetizations [12]. In $Ni_{1.2}Mn_{1.8}BO_5$ the Mn ions occupy all four metallic sites leading to a high degree of positional disorder and to the formation of interacting subsystems which could have different temperature dependencies on magnetization [10].

For the $Ni_2M'O_2BO_3$ ludwigites, with M' being a nonmagnetic ion, studies of their magnetic properties were performed only for two ludwigites: $Ni_5Ge(O_2BO_3)_2$ [13] and $Ni_5Sn(O_2BO_3)_2$ [14]. In $Ni_5Ge(O_2BO_3)_2$, the competition between antiferromagnetic and ferromagnetic exchange interactions weakened by the presence of the nonmagnetic Ge seems to give rise to magnetic frustration. In spite of the presence of a peak in the specific heat at the same temperature at which the magnetization rises sharply (∼87 K) the authors of Ref. [13] interpreted these anomalies as indicating a partial ordering or spin-glass state. In a similar way, the ludwigite $Ni_5Sn(O_2BO_3)_2$ exhibits partial magnetic order at 73 K but no long-range magnetic order of the whole system was observed at lower temperatures [14]. At ∼15 K a reordering or ordering of another subsystem may take place [14].

The main difference between $Ni_5Ge(O_2BO_3)_2$ and $Ni_5Sn(O_2BO_3)_2$ is the distribution of nonmagnetic ions at site 4. While Ge occupies randomly site 4, the Sn alternates its position at site 4 with Ni along the c axis. Thus, the difference in magnetic properties of these two compounds could be related to the ordered or disordered distribution of the nonmagnetic ions at site 4. In $Co_5Sn(O_2BO_3)_2$ ludwigite, the nonmagnetic ion Sn strengthens the magnetic interactions, and long-range magnetic order is observed due to the absence of the double-exchange interaction [4]. On the other hand, the situation is completely different for the $Ni_2M'O_2BO_3$ ludwigites, where nickel has a unique valence state (2+) and consequently no double-exchange interactions is expected. Since long-range magnetic order has not been observed in these compounds, it seems that, in this case, the diamagnetic ion plays a completely different role than in the Co ludwigites.

To better understand the role of superexchange interactions, spin size, and of the order or disorder of the nonmagnetic ions at site 4 in the ludwigites of Ni, we synthesized a $Ni_5Ti(O_2BO_3)_2$ ludwigite single crystal. Notice that, up to now in the literature there is only information about its crystalline structure [16]. X-ray experiments presented here confirm the formation of the ludwigite structure and show that Ti ions occupy randomly site 4.

Through bond valence sum (BVS) calculations and the analysis of the magnetization data, it was possible to attribute an oxidation state 2+ and spin $S = 1$ for all Ni ions in $Ni_5Ti(O_2BO_3)_2$. The magnetization and specific-heat results shown below indicate a partial magnetic ordering at 92 K and that, below 78 K, all magnetic ions are ordered. This total ordering is thus observed in a Ni ludwigite.

II. EXPERIMENT

A. Sample preparation

The crystals were synthesized from a 5 : 1 : 2 : 10 molar mixture of $NiO : TiO_2 : H_3BO_3 : Na_2B_4O_7$, respectively. This mixture was heated at 1150 °C for 24 hours and then cooled to 800 °C for 24 hours. Then the oven was turn off. The growth of crystals was carried out in air in a platinum crucible with lid. The final product was dissolved in hot water with a small concentration of HCl and the crystals were then cleaned in an ultrasonic bath at 50 °C. Needle-shaped black crystals up to 0.2 mm long were obtained.

B. X-ray diffraction

A single-crystal x-ray diffraction was done by using a D8 Venture Bruker diffractometer at room temperature, using an Incoatec Microfocus Source (IμS) x-ray, Mo Kα radiation. The crystal was mounted on a Kappa goniometer, and the data were collected by using a PHOTON 100 detector. Data collection was performed with APEX [17]. Multiscan correction using a multifaceted crystal model was applied. The full-matrix least-squares refinements based on F^2 with anisotropic thermal parameters were carried out by using SHELXL-2013 [18] program packages with WINGX [19] and SHELXLE [20] software interfaces.

Crystal data, data-collection parameters, and structure-refinement data are displayed in Table I. The crystallographic table was generated by using WINGX [19].

A schematic structure of the ludwigite projected along the c axis together with the polyhedra centered at metal ions is shown in Fig. 1. We remark that the complete structure, except for the boron ions, may be obtained from the two three-legged ladders subunits formed respectively by the metal sites 4-2-4 and 3-1-3. The purity of the sample was confirmed by powder x-ray diffraction and the presence of Ti in the

TABLE I. Crystal data and structure refinement of $Ni_5Ti(O_2BO_3)_2$.

Empirical formula	$Ni_{4.98}Ti_{1.02}B_2O_{10}$
Formula weight	522.85
Wavelength	0.717073 Å
Temperature	293(2) K
Crystal system	Orthorhombic
Space group	*Pbam*
Unit-cell dimension $a =$	9.1935(2) Å
$b =$	12.2172(3) Å
$c =$	2.99390(10) Å
Volume	336.271(16) $Å^3$
Z	2
Density (calculated)	5.164 Mg/m^3
Crystal size (μm^3)	$200 \times 50 \times 30$
Absorption coefficient	14.865 mm^{-1}
$F(000)$	504
θ range (degrees)	2.773 to 35.062
Index range $h =$	−14, 14
$k =$	−19, 19
$l =$	−4, 4
Reflections collected	37483
Independent reflections	858
R(int)	0.1088
Completeness to $\theta = 25.242$	100%
Refinement method	Full-matrix least squares on F^2
Data, restraints, parameters	858, 0, 61
Goodness-of-fit on F^2	1.151
Final R indices $[I > 2\sigma(I)]$	$R1 = 0.0206$, $wR2 = 0.0478$
R indices (all data)	$R1 = 0.0235$, $wR2 = 0.0492$
Extinction coefficient	0.0279(14)
Largest diff. peak	0.675 e $Å^{-3}$
Largest diff. hole	−0.806 e $Å^{-3}$

compound by energy-dispersive x-ray spectroscopy (EDS) (data not shown). As indicated in Table I, the space group of $Ni_5Ti(O_2BO_3)_2$ is *Pbam* and the calculated lattice parameters are in close agreement with those found in Ref. [16]. The sites 1, 2, and 3 are exclusively occupied by Ni atoms. Site 4 is occupied randomly by Ni and Ti ions at almost the same proportion (0.49 to 0.51). No evidence for an ordered distribution of the Ti at site 4 was observed. From the x-ray analysis we arrived at the chemical composition for our compound: $Ni_{4.98}Ti_{1.02}(O_2BO_3)_2$, which will be referred to as $Ni_5Ti(O_2BO_3)_2$. Table II shows the fractional coordinates and the site-occupation factor.

The intermetallic distances in this compound are shown in Table III. For comparison, the same distances for $Ni_5Ge(O_2BO_3)_2$ and $Ni_5Sn(O_2BO_3)_2$ are also shown. As we can see, the intermetallic distances for the three compounds are almost the same. The chemical bond angles M–O–M, which are important to discuss superexchange magnetic interactions, are quite different in the two three-legged-ladder subunits. In the following, for a given Ni ion with nearly equal Ni–O–Ni bond angles, only its average value will be given. The Ni (Ti) at site 4 is bonded, through the oxygen, to 11 metal ions, where seven bond angles are 94.6°, two are 118.3°, and two are 165.7°. Analogously, the Ni (Ti) at

TABLE II. Atomic coordinates and site-occupation factor (SOF) for $Ni_5Ti(O_2BO_3)_2$. $U(eq)$ is defined as one third of the trace of the orthogonalized U_{ij} tensor.

Site	x/a	y/b	z/c	SOF	$U(eq)$
Ni(1)	1	1/2	0	1/4	5(1)
Ni(2)	1	0	−1/2	1/4	6(1)
Ni(3)	0.9995(1)	0.2174(1)	0	1/2	5(1)
Ni(4)	0.7403(9)	0.1146(7)	−1/2	0.51	4(1)
Ti(4)	0.7383(12)	0.1136(9)	−1/2	0.49	4(1)
O(1)	1.1085(2)	0.3557(1)	0	1/2	8(1)
O(2)	0.8479(2)	0.2620(1)	−1/2	1/2	6(1)
O(3)	0.8822(2)	0.0762(1)	0	1/2	8(1)
O(4)	0.8498(2)	0.4580(1)	−1/2	1/2	6(1)
O(5)	1.1236(2)	0.1408(1)	−1/2	1/2	6(1)
B	0.7727(2)	0.3600(2)	−1/2	1/2	5(1)

site 2 has eight (four) bond angles at 89.7° (165.4°). The Ni at site 1 has six and two bond angles at 93.8° and 119.8°, respectively. Finally, the Ni at site 3 has six and three bond angles at 94.1° and 118.8°, respectively. In all the cases, the smaller (larger) angles correspond to the nearest-neighbor (next-nearest-neighbor) Ni ions. Sites 2 and 4 have the larger bond angles (165.7°), with site 4 possessing four of them. Thus, it is expected that stronger magnetic interactions take place at 4-2-4 three-legged ladders.

From the Ni–O distances, we can estimate the oxidation numbers for the Ni ions in each crystallographic site by using the bond valence sum (BVS) calculations [21]. We applied the formulas given by Liu and Thorp [21] for the oxidation number Z_j for the Ni ion on site j:

$$Z_j = \sum_j s_{ij}, \tag{1}$$

where $s_{ij} = \exp[(R_0 - r_{ij}/b)]$, R_0 and b are parameters given in Ref. [21], and r_{ij} is the distance to the nearest-neighbor oxygen ions. Table IV shows the results for oxidation numbers

TABLE III. The $d_{j\text{-}k}$ bond lengths (Å) between metallic ions in heterometallic ludwigites of Ni, where j, k are the crystallographic positions. The subscript is the symmetry code (i) x, y, $z+1$. The lattice parameters (Å) and the volume of the unit cell ($Å^3$) are also displayed.

$d_{j\text{-}k}$	$Ni_5Ge(O_2BO_3)_2$ [13]	$Ni_5Sn(O_2BO_3)_2$ [14,22]	$Ni_5Ti(O_2BO_3)_2$
$d_{j\text{-}j}$	2.98	3.0446(10)	2.9939(11)
$d_{4\text{-}3}$	3.084	3.131(4)	3.1010(10)
$d_{4\text{-}3i}$	3.344	3.372(4)	3.365(10)
$d_{2\text{-}3}$	3.049	3.056(4)	3.0487(3)
$d_{4\text{-}2}$	2.763	2.875(5)	2.7780(12)
$d_{4\text{-}1}$	3.003	3.045(3)	2.9940(10)
$d_{1\text{-}3}$	3.411	3.4717(13)	3.4527(3)
a	9.18	9.301	9.1935(2)
b	12.14	12.275	12.2172(3)
c	2.98	6.102	2.99390(10)
V	332.62	347.77	336.271(16)

TABLE IV. Oxidation numbers for the Nickel ions in $Ni_5Ti(O_2BO_3)_2$ obtained by using the bond valence sum (BVS) [21].

Ni_1	2.016
Ni_2	2.054
Ni_3	2.045
Ni_4	2.330

Z_j. From these results we can ascribe a valence 2+ to all nickel ions. This result shows that, for a correct electronic balance, the Ti atoms must adopt a nonmagnetic oxidation state +4. For the Ni at site 4 the oxidation number Z_j is slightly larger than that for the other sites, which may be related to the fact that sites 4 involve edge-sharing TiO_6 and NiO_6 octahedra.

Features involving structural transitions and changes in ludwigites seem to be correlated with charge ordering in mixed valence homometallic ludwigites [3,23]. In $Ni_5Ti(O_2BO_3)_2$ the Ni ions have a unique valence state (2+) and structural changes, in principle, are unexpected.

C. Magnetic measurements

The magnetic measurements were performed on powdered samples of $Ni_5Ti(O_2BO_3)_2$ by using a commercial PPMS platform from Quantum Design. Figure 2 shows the temperature dependence of the magnetization curves for zero-field-cooled (ZFC) and field-cooled (FC) processes, with an applied magnetic field of 100 Oe. Upon lowering the temperature, a small but appreciable increase in magnetization occurs below 92 K, indicating the onset of a magnetic transition. Upon further cooling to 78 K, a more pronounced increase in magnetization is clearly observed and the ZFC and FC curves diverge.

For lower temperatures, the magnetization in zero-field cooling decreases, indicating that the ordered magnetic system breaks down in magnetic domains, consistent with the observation of dissipation in the imaginary part of the AC susceptibility (not shown).

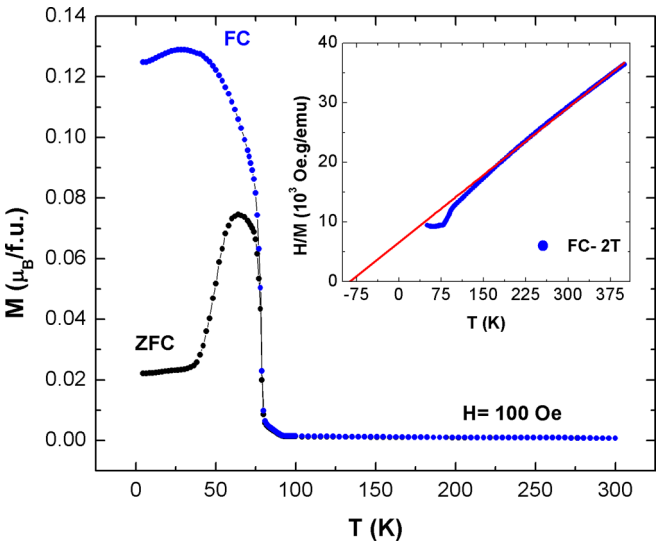

FIG. 2. Magnetization versus temperature for $Ni_5Ti(O_2BO_3)_2$ ludwigite under an applied magnetic field of 100 Oe. Inset shows inverse magnetization in a 2 T magnetic field.

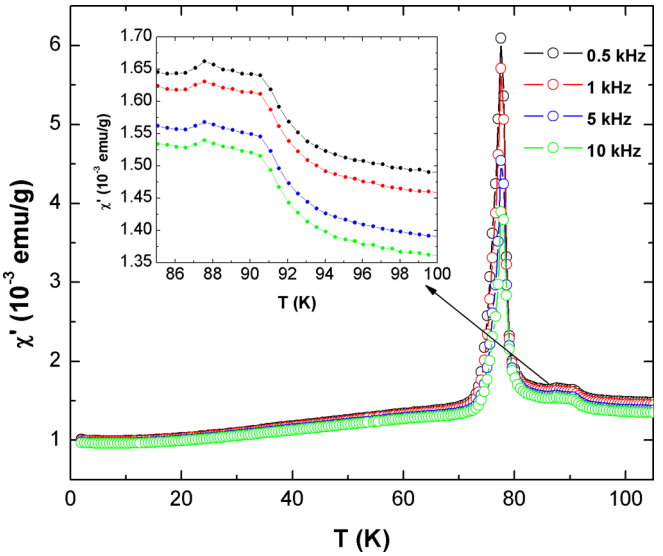

FIG. 3. Real part of $Ni_5Ti(O_2BO_3)_2$ AC magnetic susceptibility as functions of temperature for 0.5, 1, 5, and 10 kHz. The amplitude of the oscillating magnetic field is 10 Oe.

The inset shows the temperature dependence of the inverse of the susceptibility, which is linear above 150 K and can be well described by the Curie-Weiss law. From the Curie-Weiss law fitting (see inset) we obtain a Curie constant $C = 13.30 \times 10^{-3}$ emu K Oe^{-1} g^{-1} and a Curie-Weiss temperature $\Theta_{CW} = -87.91$ K. These results indicate the predominance of antiferromagnetic interactions. Using the Curie constant we determine the effective moment per Ni atom, $3.34\mu_B$, a value consistent with those observed ($3.2\mu_B$) [24] for Ni^{2+} with $S = 1$.

Figure 3 shows the real part of the AC susceptibility χ' as a function of temperature and for different frequencies. There we can observe a rather broadened peak close to 92 K (see Fig. 3), the same temperature at which a spontaneous magnetization was observed in the ZFC and FC magnetization curves. Concomitant with the magnetization results, the AC susceptibility measurements show a sharp peak at 78 K. The position of the peak does not change with the frequency, indicating well-defined magnetic ordering.

Figure 4 shows hysteresis curves for different temperatures. Above 100 K the hysteresis loops are closed, which is typical of a paramagnetic state. Below 92 K the hysteresis loops open with both the coercive field and the remanent magnetization increasing as the temperature decreases. At temperatures between 92 and 80 K, the hysteresis curves are discontinuous and present *steps*. In Fig. 5 we can see a step near the magnetic field of 1 T. This behavior is best observed in the derivative of the magnetization (see inset of Fig. 5). Below 78 K, the steps in the hysteresis curves are no longer observed. A maximum coercive field of ~0.8 T and remanent magnetization of ~$0.13\mu_B$ per unit formula is achieved at 4.5 K. The existence of a remaining magnetization indicates a ferromagnetic or ferrimagnetic component of the magnetic

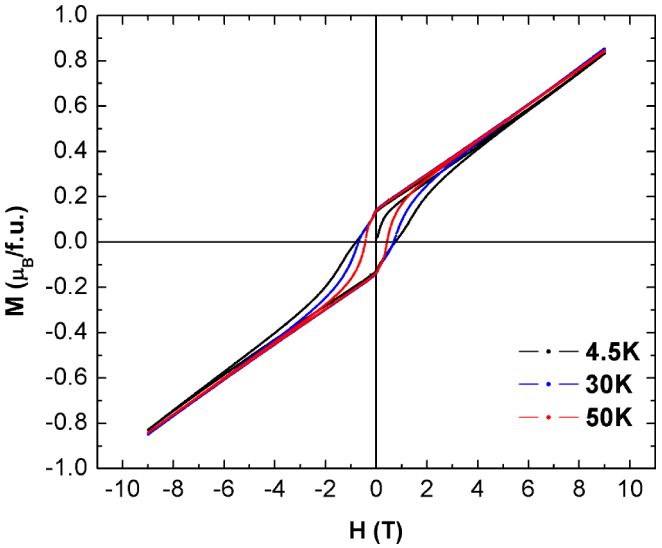

FIG. 4. Hysteresis loops for the powdered $Ni_5Ti(O_2BO_3)_2$ compound at 4.5, 30, and 50 K.

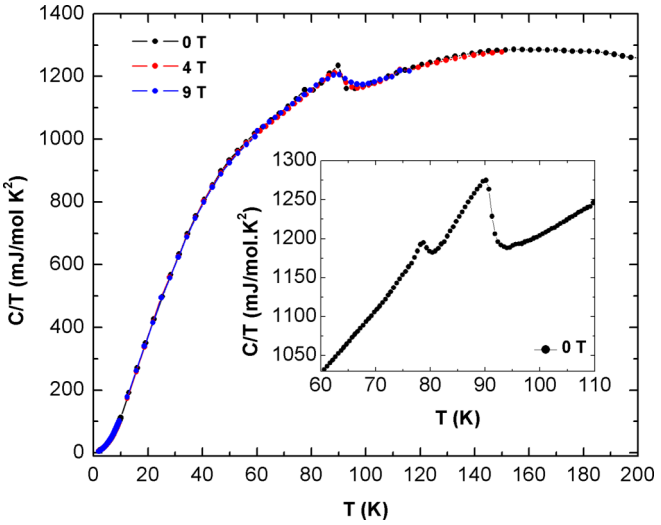

FIG. 6. Specific heat of $Ni_5Ti(O_2BO_3)_2$ represented as C/T versus T for 0, 4, and 9 T fields. Inset shows a zoom of the region where the magnetic transitions take place.

moments of Ni. Even at 4 K and 9 T it was not possible to reach complete magnetic saturation indicating probably due to anisotropy effects.

D. Specific-heat measurements

Specific-heat measurements as functions of temperature and external applied magnetic fields were performed on a polycrystalline sample and are shown in Fig. 6. In zero external magnetic field a well-defined peak is observed at ∼92 K, the same temperature at which an anomaly is observed in the magnetization curves. Furthermore, although not so obvious, a perceptible shoulder is observed at 78 K (see inset of Fig. 6).

The low-temperature ($T < 9$ K) specific-heat data were best analyzed by using the power law $C = \gamma T + \beta T^3$. The parameters obtained from the fittings are presented in Table V (see also Fig. 7).

As it is well known, the T^3 term in solids is usually due to elastic excitations (phonons) and the β parameter is related to the effective Debye temperature Θ_D through the equation

$$\Theta_D^3 = 234\frac{R}{\beta}, \tag{2}$$

where R is the universal gas constant. Θ_D values calculated for $Ni_5Ti(O_2BO_3)_2$ are shown in Table V. For comparison, Θ_D values for other ludwigites are also shown. Notice in this table that the values of β are field independent, which confirms the elastic nature of the modes responsible for this contribution. Indeed, in three-dimensional antiferromagnets with low anisotropy the magnetic excitations (magnons) have a linear dispersion relation that also gives rise to a T^3 contribution to the specific heat. The independence of the coefficient β on the external field rules out this possibility.

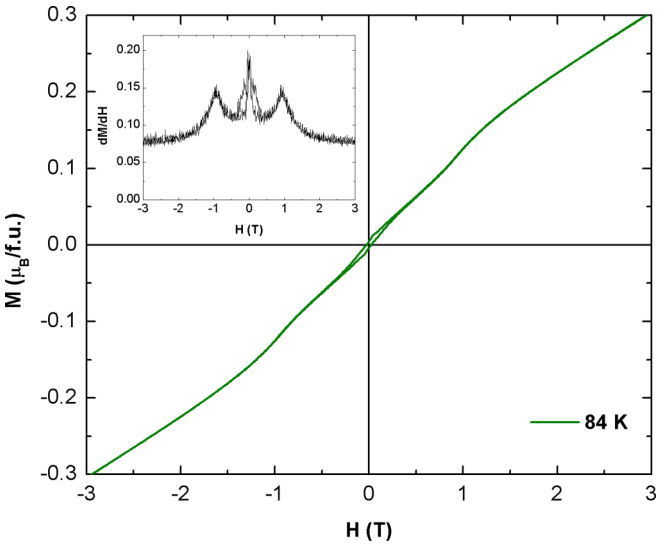

FIG. 5. Hysteresis loop for the powdered $Ni_5Ti(O_2BO_3)_2$ compound at 84 K. Inset shows the derivative of the field dependence of the magnetization.

TABLE V. Parameters γ and β obtained from the fitting ($C = \gamma T + \beta T^3$) of the low-temperature specific-heat data (Fig. 7) of the ludwigite $Ni_5Ti(O_2BO_3)_2$. Calculated Debye temperatures Θ_D are also shown. "PW" stands for "present work."

	H (T)	γ (mJ mol^{-1} K^{-2})	β (mJ mol^{-1} K^{-4})	Θ_D (K)	Ref.
$Ni_5Ti(O_2BO_3)_2$	0	2.259 ± 0.028	1.027 ± 0.001	124	PW
$Ni_5Ti(O_2BO_3)_2$	4	1.714 ± 0.021	1.044 ± 0.001	123	PW
$Ni_5Ti(O_2BO_3)_2$	9	1.188 ± 0.019	1.097 ± 0.001	121	PW
$Ni_5Ge(O_2BO_3)_2$	0	1.7	0.52	155	[13]
$Ni_5Ge(O_2BO_3)_2$	2.5	3.8	0.49	158	[13]
$Co_5Ti(O_2BO_3)_2$	0	15.5	3.94	79	[5]
$Co_5Ti(O_2BO_3)_2$	3	6.88	2.78	89	[5]
$Co_5Ti(O_2BO_3)_2$	9	3.61	2.76	89	[5]
$Co_5Sn(O_2BO_3)_2$	0	0.54	0.65	144	[4]
$Co_5Sn(O_2BO_3)_2$	9	0.00	0.66	143	[4]

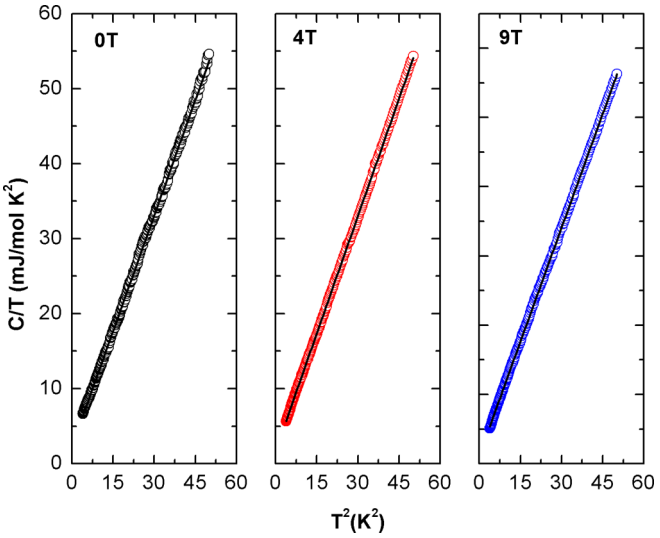

FIG. 7. Specific heat of $Ni_5Ti(O_2BO_3)_2$ represented as C/T versus T^2 for 0, 4, and 9 T fields. The parameters of the linear fittings are shown in Table V.

The linear term is usually attributed to the electronic contribution (free electrons in a Fermi liquid). Oxyborates are semiconductors at low temperatures, but this term could arise from traveling electrons in the three-legged ladder in mixed-valence homometallic ludwigites, as in the case of $Co_3B_2O_5$, where Co^{2+} and Co^{3+} are present, or $Fe_3B_2O_5$ with Fe^{2+} and Fe^{3+} charge states [1]. A linear temperature dependence of the specific heat is also observed in spin glasses with magnetic frustration. The γ value found here is small when compared, for example, with $Co_5Ti(B_2O_3)_2$ [5], which behaves as a conventional spin glass. It is similar to that found in the ludwigite $Co_5Sn(B_2O_3)_2$ [4], where long-range magnetic order takes place at 82 K.

According to single-crystal x-ray diffraction results $Ni_5Ti(O_2BO_3)_2$ has only Ni^{2+} ions (see Table IV), so an electronic contribution to the linear term of the specific heat due to mixed valence is expected to be negligible. The linear term is partially suppressed by an external magnetic field, as shown in Table V, and we attribute its origin to magnetic frustration, which is common in spin-glass materials. The small values of γ indicate a lower degree of frustration in the present system when compared with the other ludwigites (see Table V). This is in agreement with the ratio Θ_{CW}/T_N, with $\Theta_{CW} = -87.91$ K and T_N taken either as 92 or 78 K, being not too far from unity. This shows that there are fewer competing interactions in $Ni_5Ti(O_2BO_3)_2$.

III. DISCUSSION

Single-crystal x-ray diffraction results have shown that in $Ni_5Ti(O_2BO_3)_2$ the Ti ions occupy only sites 4 of the structure. So, sites 4 are randomly occupied by Ti and Ni ions in the ratio 1 : 1. BSV calculations allowed us to attribute a 2+ valence state to all Ni ions. As a consequence, the Ti ions must adopt the nonmagnetic 4+ valence state for a correct charge balance. Thus, on average, a 3+ valence for site 4, as found in the ludwigites of Fe [3] and Co [8], also seems to be characteristic of the ludwigites containing Ni as the metallic ion [6].

In ludwigites there is a competition between three types of magnetic interactions, direct-, super-, and double-exchange, which leads to a variety of magnetic properties exhibited by these compounds [3–5,7,8]. Neutron experiments indicate that, in the 4-2-4 three-legged ladders of $Fe_3O_2BO_3$, the 180° bond angle antiferromagnetic superexchange interactions is stronger than the others; namely, 90° superexchange, double-, and direct-exchange interactions. In $Fe_3O_2BO_3$ the presence of LS Co^{3+} in the two lateral legs of the 4-2-4 three legged ladders give place to a ferromagnetic order of the central leg of these ladders [8]. However, a simple superexchange-interaction calculation considering all Co ions in the 4-2-4 three-legged ladders to be magnetic indicates that the 180° antiferromagnetic superexchange interaction should also be dominant [25].

In $Ni_5Ti(O_2BO_3)_2$, where the only magnetic ions are the Ni^{2+} with $S = 1$, the double-exchange interaction is excluded. Furthermore, the direct interaction between Ni^{2+} ions with edge-sharing octahedra involving only e_g orbitals is negligible [26,27]. Thus, the superexchange interaction seems to play a crucial role in determining the magnetic structure of the $Ni_5Ti(O_2BO_3)_2$. The shortest distance between two Ni ions is found in the ladder 4-2-4 ($d_{4-2} = 2.778$ Å). Thus, it is there where the strongest magnetic interactions are expected to occur. In NiO ($T_N = 523$ K) [28], where the shortest distance between Ni ions ($d = 2.954$) is comparable to that found in the 4-2-4 ladder of $Ni_5Ti(O_2BO_3)_2$, the ferromagnetic 90° Ni^{2+}–O–Ni^{2+} superexchange interaction is weak and the direct exchange does not play any important role [27]. On the other hand, ^{119}Sn Mössbauer spectroscopy has shown that the 180° Ni^{2+}–O–Ni^{2+} indirect exchange couplings involving the e_g orbitals are strongly antiferromagnetic and dominant [29].

In $NiTiO_3$, where Ni^{2+} magnetic layers are separated by nonmagnetic layers formed by Ti^{4+}, the shortest distance between two Ni ions is $d = 2.9485$ Å and involves only ferromagnetic 90° Ni^{2+}–O–Ni^{2+} superexchange interactions [30]. This compound undergoes a long-range magnetic order at 23 K with a ferromagnetic spin structure within the layers which are antiferromagnetically stacked along the [111] direction [30].

Calculations of exchange integrals for the $Ni_5Ge(O_2BO_3)_2$ have also shown that the superexchange for a 180° Ni^{2+}–O–Ni^{2+} bond is strong and antiferromagnetic while the superexchanges for 90° bonds are weaker and ferromagnetic [13]. Superexchanges for 120° are less significant and antiferromagnetic.

Recent studies in the hulsite $Ni_5Sn(O_2BO_3)_2$ have shown that, for Ni atoms positioned in a quadrangular arrangement, the bond angles and separation between the Ni ions are almost the same as those found in the 4-2-4 ladder of the $Ni_5Ti(O_2BO_3)_2$ ludwigite. In this case, the ^{119}Sn Mössbauer results have shown that the superexchange interactions are strong and antiferromagnetic [31], comparable only to the interactions in the NiO compound [29].

Due to the random distribution of Ti^{4+} atoms at sites 4, it is realistic to assume that there are Ni-rich regions in the 4-2-4 ladder of $Ni_5Ti(O_2BO_3)_2$. Probably, these regions are not many, but they are enough to percolate and give rise to magnetic order. In these regions the Ni ions have a

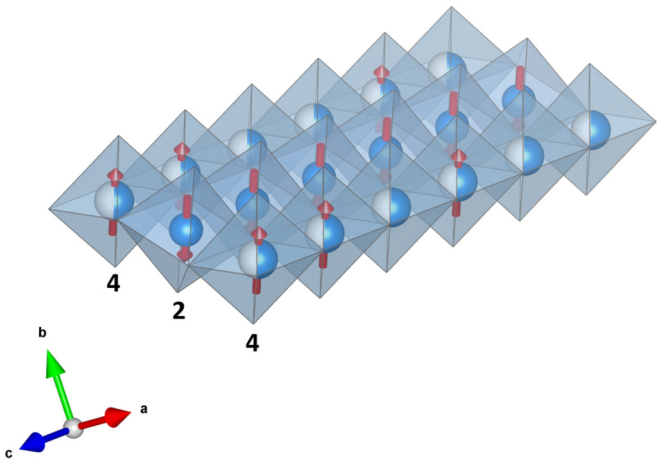

FIG. 8. Proposed magnetic structure for the 4-2-4 ladder showing Ni-rich regions. This structure is consistent with the Goodenough-Kanamori rules because all 180° Ni^{2+}–O–Ni^{2+} bonds are antiferromagnetic in this way. The figure was generated by VESTA software [15].

165.7° Ni^{2+}–O–Ni^{2+} exchange bond angle and antiferromagnetic superexchange interactions are expected to be strong and dominant, as pointed out by the negative Curie-Weiss temperature, $\Theta_{CW} = -87.91$ K. An antiferromagnetic spin structure for the Ni-rich regions in the 4-2-4 ladder dominated by antiferromagnetic (AFM) superexchange interactions is shown in Fig. 8. This type of magnetic structure is found in NiO oxide with 180° exchange bond angle and in $Ni_5Sn(O_2BO_3)_2$ hulsite wherein the Ni ions have the same distance and bond angles that the Ni ions have in the 4-2-4 ladders of $Ni_5Ti(O_2BO_3)_2$. Thus, the anomalies observed in the magnetization, susceptibility, and specific-heat measurements at 92 K could be attributed to a magnetic ordering of Ni-rich regions of the 4-2-4 ladders. The slightly open hysteresis loops at 90 K are compatible with the magnetic structure shown in Fig. 8, where an antiferromagnetic ordering results in a ferromagnetic component.

Below 90 K another inflection point at ∼78 K is observed in the temperature dependence of the susceptibility. The presence of two inflection points in the susceptibility curve (see inset of Fig. 3) and the appearance of stairs in the hysteresis loops at temperatures between 80 and 92 K (see Fig. 5) are compatible with the existence of loosely coupled magnetic subsystems being ordered separately at different temperatures. This assumption is realistic if we think that, for the stoichiometric balance of the 4-2-4 ladder, there will be regions with lower or higher Ti content at site 4. In these regions, the Ni ions will be loosely coupled due to the presence of the nonmagnetic Ti ions that weakens the magnetic interactions, as in the $Co_5Ti(O_2BO_3)_2$ ludwigite [5]. Obviously, we cannot rule out clusters with high concentrations of Ti at site 4 that can lead to small regions with a magnetic disorder or spin-glass state.

At 78 K, a large increase in magnetic susceptibility and a second small peak in the temperature dependence of the specific heat indicates a new magnetic transition, which we attribute to the magnetic ordering of the remaining Ni ions at sites 3-1-3 of the $Ni_5Ti(O_2BO_3)_2$. These ions, together with those in the 4-2-4 ladders, form a new magnetic structure. The position of the peak in the magnetic susceptibility does not shift with frequency, showing that this is a genuine magnetic phase transition and not a freezing of the magnetic moments. This is further supported by the presence of the anomaly in the low-temperature specific-heat measurements.

The small γ parameter for $Ni_5Ti(O_2BO_3)_2$, which is somewhat affected by the applied magnetic field (see Table V), corroborates a feeble competition between the magnetic interactions and consequently weak frustration. The linear contribution to the specific heat with a small γ coefficient could originate from small regions of the 4-2-4 ladders with magnetic frustration due to the presence of Ti ions.

Thus, the magnetism of $Ni_5Ti(O_2BO_3)_2$ is governed essentially by superexchange interactions. This seems to reduce competition and reinforces long-range magnetic order. Despite the negative value of Θ_{CW} and the 165.7° superexchange bond angles indicating a predominance of antiferromagnetic interactions, the magnetic ground state is not a conventional antiferromagnetic due to the presence of low-dimensional units in the form of three-legged ladders in the crystalline structure. The low-temperature hysteresis curves point to a magnetic order with a structure, such that a ferromagnetic component results. Neutron-diffraction studies are being planned to elucidate the spin structure of this compound.

Considering the structural features of the $Ni_5Ti(O_2BO_3)_2$ and $Ni_5Ge(O_2BO_3)_2$, which have almost the same interatomic distances and chemical bonding angles, they should, in principle, exhibit very similar magnetic properties. However, for an adequate comparison of the magnetic properties of these two compounds it would be convenient to have additional information about the magnetic susceptibility of $Ni_5Ge(O_2BO_3)_2$. In addition, other details related to the exchange interactions also have to be taken into account, such as, for example, the more distant exchange interactions, such as interactions of the type Ni^{2+}-O-*A*-O-Ni^{2+}, in which *A* denotes a diamagnetic cation. These interactions depend on the geometrical configuration of the path, the kind of diamagnetic ions intervening in the path, and so on. They are generally neglected; however, in these compounds it may play a crucial role in the establishment of long-range magnetic order. The magnetic transition temperature of the $Ni_5Ti(O_2BO_3)_2$ is slightly higher than that of the $Ni_5Ge(O_2BO_3)_2$ and, if we consider that the ionic radius for Ti^{4+} (0.605 Å) is much larger than that for Ge^{4+}(0.53 Å), it could be inferred that the most distant exchange interactions play a more effective role in the case of Ti^{4+} than in the case of Ge^{4+} as concerns the appearance of long-range magnetic order. For a comparison with $Ni_5Sn(O_2BO_3)_2$, where Sn^{4+} has even a larger ionic radius (0.69 Å), other additional parameters such as the positional symmetry of the Sn ions in the 4-2-4 ladder should be taken into account. Studies of Ni ludwigites doped with other nonmagnetic ions will be performed to understand how the diamagnetic cations affect the more distant exchange interactions and their role in the establishment of a long-range magnetic order.

IV. CONCLUSIONS

X-ray experiments show that, in $Ni_5Ti(O_2BO_3)_2$, sites 4 are randomly shared, in a 1 : 1 ratio, by Ni and Ti ions. The

interatomic distances allowed us to ascribe a valence 2+ to all Ni ions. Magnetization and specific-heat experiments are consistent with long-range magnetic order at low temperatures for the $Ni_5Ti(O_2BO_3)_2$ ludwigite. This ordering is achieved in several stages as the temperature is lowered. The 92 K anomalies observed in the temperature dependence of the magnetization and specific-heat data are attributed to partial magnetic ordering of the 4-2-4 ladders. In these ladders, the strongest exchange interactions take place due to the proximity between the Ni ions and to the existence of chemical bond angles close to 180°. They contain dominant antiferromagnetic exchange interactions and strong *d*-*d* overlap. Below 78 K, the spins of the remaining Ni ions at sites 1 and 3 order magnetically to form, together with the 4-2-4 ladder, a ferrimagnetic-type structure. The small value found for the γ parameter may be related to the existence of magnetically disordered regions due to the magnetic frustration caused by the presence of the nonmagnetic Ti^{4+} ion.

ACKNOWLEDGMENTS

Support from LDRX-UFF and the Brazilian agencies CAPES, CNPq, and FAPERJ is gratefully acknowledged.

[1] A. Narlikar, *Frontiers in Magnetic Materials* (Springer-Verlag, Berlin, Heidelberg, 2005).
[2] S. Sofronova and I. Nazarenko, Cryst. Res. Technol. **52**, 1600338 (2017).
[3] P. Bordet and E. Suard, Phys. Rev. B **79**, 144408 (2009).
[4] C. P. C. Medrano, D. C. Freitas, D. R. Sanchez, C. B. Pinheiro, G. G. Eslava, L. Ghivelder, and M. A. Continentino, Phys. Rev. B **91**, 054402 (2015).
[5] D. C. Freitas, R. B. Guimarães, D. R. Sanchez, J. C. Fernandes, M. A. Continentino, J. Ellena, A. Kitada, H. Kageyama, A. Matsuo, K. Kindo *et al.*, Phys. Rev. B **81**, 024432 (2010).
[6] D. C. Freitas, M. A. Continentino, R. B. Guimarães, J. C. Fernandes, E. P. Oliveira, R. E. Santelli, J. Ellena, G. G. Eslava, and L. Ghivelder, Phys. Rev. B **79**, 134437 (2009).
[7] C. P. C. Medrano, D. C. Freitas, E. C. Passamani, C. B. Pinheiro, E. Baggio-Saitovitch, M. A. Continentino, and D. R. Sanchez, Phys. Rev. B **95**, 214419 (2017).
[8] D. C. Freitas, C. P. C. Medrano, D. R. Sanchez, M. N. Regueiro, J. A. Rodríguez-Velamazán, and M. A. Continentino, Phys. Rev. B **94**, 174409 (2016).
[9] N. B. Ivanova, M. S. Platunov, Y. V. Knyazev, N. V. Kazak, L. N. Bezmaternykh, E. V. Eremin, and A. D. Vasiliev, Low Temp. Phys. **38**, 172 (2012).
[10] E. Moshkina, S. Sofronova, A. Veligzhanin, M. Molokeev, I. Nazarenko, E. Eremin, and L. Bezmaternykh, J. Magn. Magn. Mater. **402**, 69 (2016).
[11] L. Bezmaternykh, E. Kolesnikova, E. Eremin, S. Sofronova, N. Volkov, and M. Molokeev, J. Magn. Magn. Mater. **364**, 55 (2014).
[12] H. Kageyama, D. I. Khomskii, R. Z. Levitin, and A. N. Vasil'ev, Phys. Rev. B **67**, 224422 (2003).
[13] S. Sofronova, L. Bezmaternykh, E. Eremin, I. Nazarenko, N. Volkov, A. Kartashev, and E. Moshkina, J. Magn. Magn. Mater. **401**, 217 (2016).
[14] S. Sofronova, L. Bezmaternykh, E. Eremin, A. Chernyshov, and A. Bovina, Phys. Status Solidi B **255**, 1800281 (2018).
[15] K. Momma and F. Izumi, J. Appl. Crystallogr. **44**, 1272 (2011).
[16] C. Stenger, G. Verschoor, and D. Ijdo, Mater. Res. Bull. **8**, 1285 (1973).
[17] APEX3, version 2017.3-0, Bruker AXS Inc., Madison, Wisconsin, USA (2017).
[18] G. M. Sheldrick, Acta Cryst. C **71**, 3 (2015).
[19] L. J. Farrugia, J. Appl. Crystallogr. **32**, 837 (1999).
[20] C. B. Hübschle, G. M. Sheldrick, and B. Dittrich, J. Appl. Crystallogr. **44**, 1281 (2011).
[21] W. Liu and H. H. Thorp, Inorg. Chem. (Washington, DC, U. S.) **32**, 4102 (1993).
[22] K. Bluhm and H. Müller-Buschbaum, Monatsh. Chem. **120**, 85 (1989).
[23] C. W. Galdino *et al.* (unpublished).
[24] J. M. D. Coey, *Magnetism and Magnetic Materials* (Cambridge University Press, 2010).
[25] N. Kazak, N. Ivanova, O. Bayukov, S. Ovchinnikov, A. Vasiliev, V. Rudenko, J. Bartolomé, A. Arauzo, and Y. Knyazev, J. Magn. Magn. Mater. **323**, 521 (2011).
[26] J. B. Goodenough, Phys. Rev. **117**, 1442 (1960).
[27] K. Motida and S. Miyahara, J. Phys. Soc. Jpn. **28**, 1188 (1970).
[28] C. G. Shull, W. A. Strauser, and E. O. Wollan, Phys. Rev. **83**, 333 (1951).
[29] V. Tkachenko, M. Korolenko, M. Danot, and P. Fabrichnyi, Russ. J. Inorg. Chem. **50**, 1247 (2005).
[30] G. Shirane, S. J. Pickart, and Y. Ishikawa, J. Phys. Soc. Jpn. **14**, 1352 (1959).
[31] C. P. C. Medrano, D. C. Freitas, E. C. Passamani, J. A. L. C. Resende, M. Alzamora, E. Granado, C. W. Galdino, E. Baggio-Saitovitch, M. A. Continentino, and D. R. Sanchez, Phys. Rev. B **98**, 054435 (2018).